

Electron microscopy of boundary structure in calcium zirconate

V. P. DRAVID, M. R. NOTIS, C. E. LYMAN

Department of Materials Science and Engineering, Lehigh University, Bethlehem, Pennsylvania 18015, USA

Various types of boundary in orthorhombic calcium zirconate (CaZrO_3) were examined using conventional transmission electron microscopy (CTEM), high-resolution electron microscopy (HREM), selected-area diffraction (SAED) and convergent-beam electron diffraction (CBED). Two types of interface, namely δ -boundaries and coherent twin boundaries were identified and analysed. The δ -boundaries were studied using CTEM, SAED and CBED; the twin boundaries were investigated using the additional technique of HREM. Pseudosymmetric twinning was observed in CaZrO_3 where the two domains were related to each other by either a 180° or a 90° rotation about an axis perpendicular to (1 0 1). A different type of twin boundary, where the adjacent domains were related by a 180° rotation about the normal to (1 0 0), was also noted. The observations are compared with previous studies on other ABO_3 -type compounds isostructural with CaZrO_3 .

1. Introduction

ABO_3 -type compounds analogous to CaZrO_3 have been extensively studied, beginning even before the discovery of X-ray diffraction. These compounds have been explored mainly because of their unique engineering properties. Despite the intense investigation that these compounds have received, there are still significant questions regarding the nature of point/space groups and the lattice parameters of some of these systems. This difficulty of obtaining unambiguous crystal structure data is chiefly attributed to the presence of fine-scale twinning and/or the unavailability of defect-free large single crystals in many ABO_3 compounds [1-6].

In this paper we report for the first time the crystallographic nature of characteristic boundaries in CaZrO_3 . The CaZrO_3 phase occurs as a stoichiometric line compound in the CaO-ZrO_2 system [7]. When the eutectic composition in this system is directionally solidified, the resultant microstructure consists of regular lamellae of CaZrO_3 and ZrO_2 (CaO-stabilized), as shown in Fig. 1. During solidification, ZrO_2 retains its defect fluorite structure but CaZrO_3 lowers its symmetry by transforming from the high-temperature cubic structure to orthorhombic structure at about 1750°C [7]. The crystal structure data for the room-temperature orthorhombic phase have not been definitively determined in the literature, but in this report we have used the lattice parameters reported by Koopmans *et al.* [3], which are

$$\begin{aligned} a &= 0.55912 \text{ nm} & b &= 0.80171 \text{ nm} \\ c &= 0.57616 \text{ nm} \end{aligned}$$

We have recently identified the space group of CaZrO_3 as Pcmm and the details of this will be published elsewhere [8].

2. Experimental procedure

The sample for the present study consisted of a eutectic microstructure containing the phases ZrO_2 (CaO-stabilized) and CaZrO_3 , as described earlier. The directional solidification conditions for this material are reported elsewhere [9]. Thin sections, transverse to the growth direction of the eutectic sample, were cut using a diamond saw and were further thinned by mechanical polishing to about $75 \mu\text{m}$. These thin discs were then thinned to perforation using a Gatan Twin Beam Ion Milling Machine operated at 6 kV and 15° incidence angle. The TEM foils were coated with a thin layer of amorphous carbon to avoid charging under the electron beam. Most of the convergent-beam electron diffraction (CBED) was performed using a Philips EM400T analytical electron microscope. A

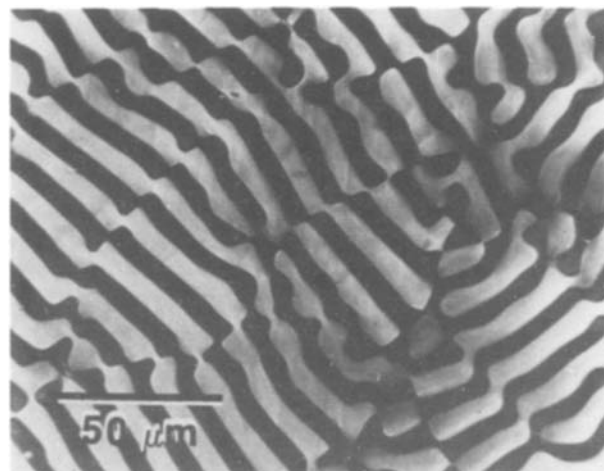
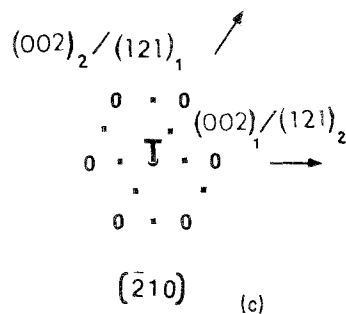
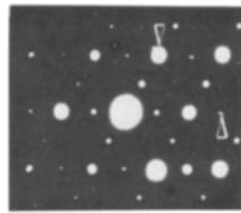
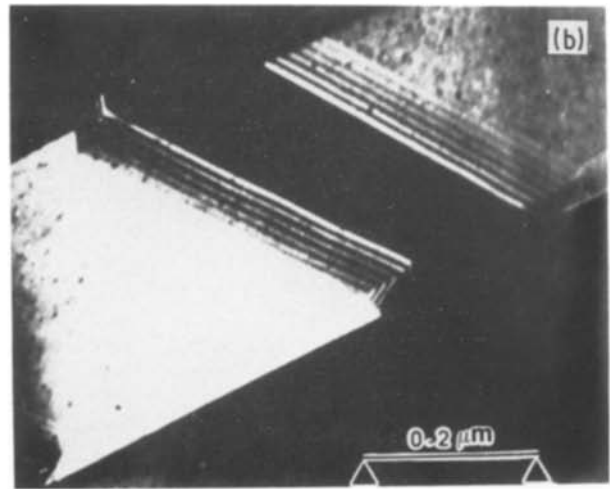
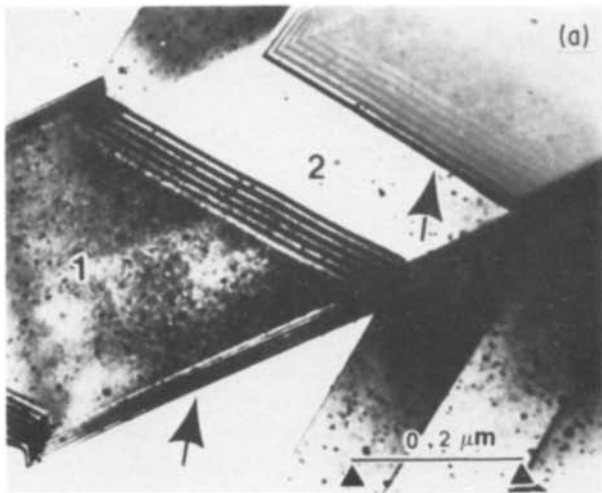


Figure 1 Transmission optical micrograph of a transverse section of CaO-ZrO_2 eutectic. The darker phase is ZrO_2 (CaO-stabilized) and the lighter phase is CaZrO_3 .



spot size of about 20 nm was used for these studies. High-resolution electron microscopy (HREM) observations were made on a Jeol JEM 2000FX microscope with a point-to-point resolution of about 0.280 nm. Although through-focal series images were taken each time, all HREM images shown in this paper were taken at near-optimum defocus.

3. Results and discussion

Figs 2a and b show, respectively, a bright-field (BF) and a centred dark-field (CDF) image of a typical boundary in the CaZrO_3 phase of the two-phase eutectic shown in Fig. 1. The BF image has asymmetrical fringe contrast (white to dark) at the interface but the CDF image using the (002) reflection from Segment 1 of the crystal shows symmetrical contrast (white to white). This contrast feature is a major characteristic of δ -boundaries.

Gevers *et al.* [10] applied the dynamical theory of electron diffraction and imaging to calculate the characteristic fringe contrast at δ -boundaries. A δ -boundary is defined by these authors as the interface separating two regions of the same crystal having slightly different values of s (deviation from the exact Bragg reflection position for a reciprocal lattice point)

Figure 2 (a) BF micrograph in the two-beam condition (g_{002} from Segment 1), showing asymmetrical fringe contrast at the interface as shown by the arrows. (b) CDF image using g_{002} from one g_{121} from two reflections. Note the symmetrical fringe contrast as opposed to the BF contrast. (c) Composite [2 1 0] zone-axis selected-area diffraction pattern Segments 1 and 2. The spot splitting (arrows) along (002)₁ and (1 2 1)₂ rows is due to the difference in lattice spacings.

or g (the Bragg reflection vector in the reciprocal lattice) for the same operative reflection in the observed electron diffraction pattern [11]. In further publications, Gevers and co-workers [12, 13] showed that δ -boundaries can be recognized in a conventional transmission electron microscope (CTEM) by the presence of asymmetrical fringe contrast in the BF image and symmetrical fringe contrast in the corresponding CDF image.

This methodology has been used by several workers to identify δ -boundaries in ferroelectric or ferromagnetic materials. BaTiO_3 is an example of a crystal where δ -boundaries arise due to differential tetragonal distortion across the boundary when the crystal goes through a perovskite-to-tetragonal transformation [12]. In the present case, the two crystal segments forming the boundary were rotated by approximately 60° about the incident beam direction (B [2 1 0]) as shown in Fig. 2c. Thus, the g_{002} reflection of Segment 1 of the crystal is almost superimposed upon the g_{121} reflection of Segment 2, as evidenced in the composite diffraction pattern shown in Fig. 2c. This leads to a spot splitting along g_{002} of one and g_{121} of two systematic rows, since the g_{002} vector of Segment 1 whose lattice spacing is 0.288 nm is just larger than g_{121} of Segment 2 whose lattice spacing is 0.284 nm. Thus, this spot splitting satisfies the requirement of a contrast effect at the δ -boundary.

There have been numerous reports in the literature concerning the characteristic twin-boundary structure in ABO_3 -type compounds. Bowman [14] studied twin systems in CaTiO_3 using optical microscopy as early as 1908. He found several twin systems in this compound which he characterized as follows: 180° rotation about a normal to (1 0 1), 90° rotation about a normal to (1 0 1), and 180° rotation about a normal to (1 2 1), all with the same compositional planes.

Recently, White *et al.* [4] studied CaTiO_3 using

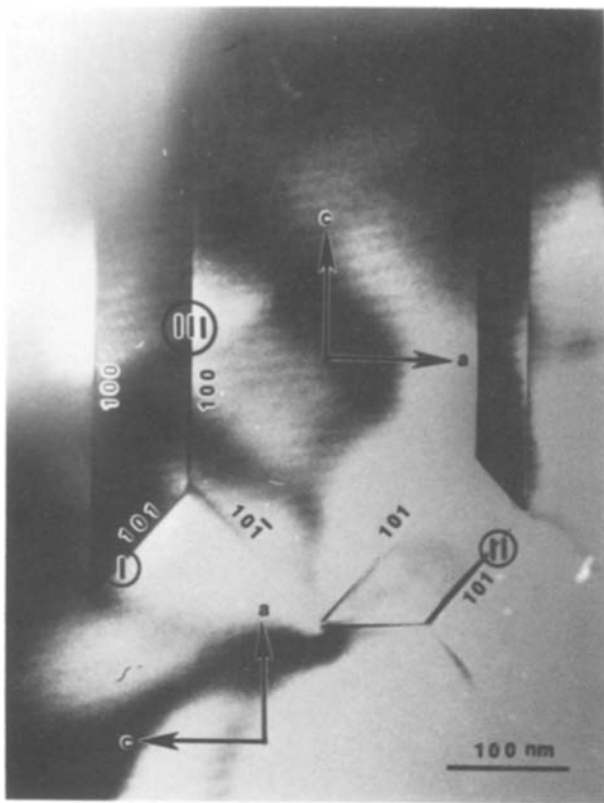


Figure 3 A BF micrograph of calcium zirconate showing different twin systems.

HREM and selected-area electron diffraction (SAED) to confirm the above twin systems. However, in addition to the twin systems reported by Bowman, they also found evidence of twinning on the (010) compositional plane. Twinning in several other systems such as CaSnO_3 and SrSnO_3 has been reported by Vegas *et al.* [5], but they did not determine the type of twinning in these systems.

Fig. 3 shows a BF image of various twin-like boundaries in CaZrO_3 . CBED was performed on individual

twin segments to reveal the crystallography associated with each twin variant. An HREM image of Area I in Fig. 3 is shown in Fig. 4. The two crystal segments separated by the boundary are related by a 90° rotation normal to a 101 compositional plane such that the *b* axis of the crystal is common to both the segments; these are designated as 90° rotation twins about (101). Note that the twin interface is almost edge-on and with no evidence of defects or the presence of a second phase. Fig. 5 shows another twin boundary (Area II in Fig. 3) which relates the adjacent crystal segments by a 180° rotation normal to (101), which is also the compositional plane. The lattice fringes are seen to run unobstructed through the interface. Such 90° and 180° twin boundaries are consistent with those observed for CaTiO_3 by several workers [4, 14, 15]. However, Kay and Bailey [15] also reported 180° twin boundaries normal to (121) in CaTiO_3 , while White *et al.* [4] observed 180° twin boundaries normal to (010). We have not observed either of these twin boundaries in our system. Instead, we have obtained evidence of 180° rotation boundaries normal to (100) as shown in Fig. 6 (Area III of Fig. 3). Note that the interface is not in edge-on configuration, and thus appears very diffuse. Also it was not possible to orient both the crystal segments at their exact zone axis; therefore, only 010 planes are imaged in this micrograph. However, it is likely that (100) and (001) twins may exist in this system though we did not observe them yet.

4. Conclusions

Two types of interface in CaZrO_3 were investigated and were identified as δ -boundaries and coherent twin boundaries. Twin relationships were determined to be either 180° or 90° rotations normal to (101). A different form of boundary with 180° rotation normal to (100) was also noted. The twin systems observed in this study appear to be consistent with twin systems investigated in compounds isostructural with CaZrO_3 .

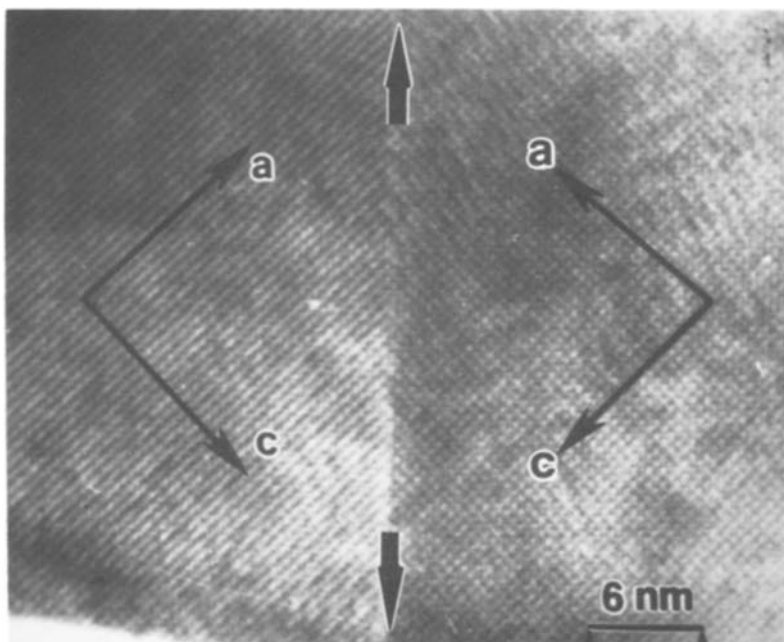


Figure 4 An HREM image of 90° rotation twin boundary (Area I in Fig. 3).

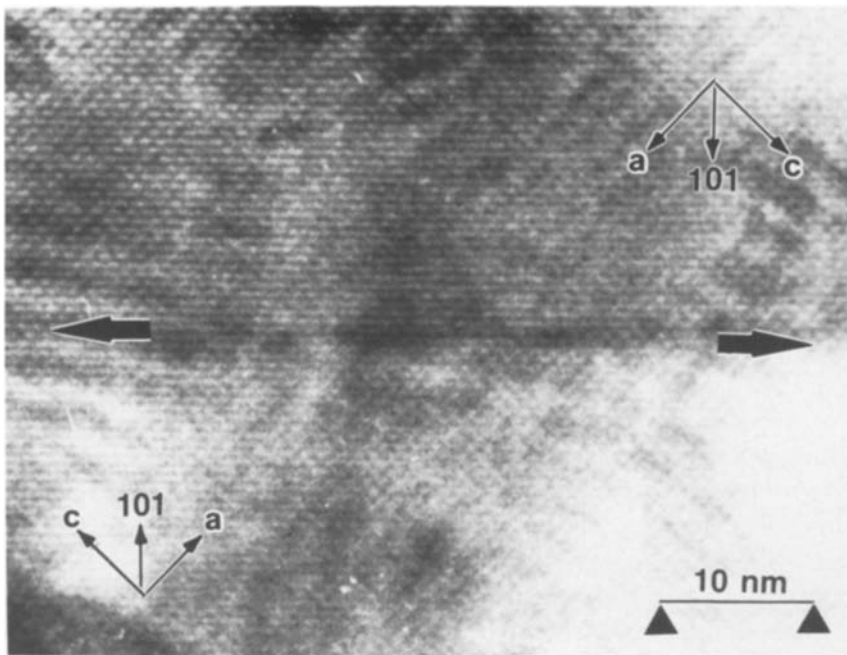


Figure 5 An HREM image of 180° rotation twin boundary (Area II in Fig. 3).

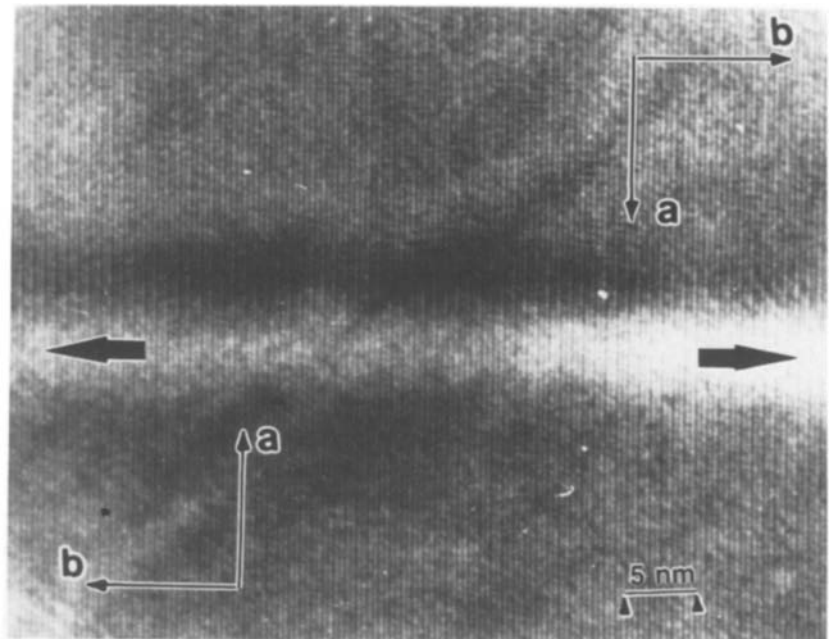


Figure 6 A lattice fringe image of 180° rotation with boundary about the normal to (100) (Area III in Fig. 3). Note the diffuse nature of the interface as opposed to Figs 5 and 6 (see text).

Acknowledgements

This study was supported by the US Department of Energy (Grant No. DEFGO2-84ER45150). We thank Professor V. S. Stubican of Pennsylvania State University for supplying the material used in this study.

References

1. H. D. MEGAW, *Proc. Phys. Soc.* **58** (2) (1946) 133.
2. R. S. ROTH, *J. Res. NBS* **58** (2) (1957) 75.
3. H. J. A. KOOPMANS, G. M. H. VAN de VELDE and P. J. GELLINGS, *Acta Crystallogr.* **C39** (1983) 1323.
4. T. J. WHITE, R. L. SEGALL, J. C. BARRY and J. L. HUTCHINSON, *ibid.* **B41** (1985) 93.
5. A. VEGAS, M. VALLET-REGI, J. M. GONZALES-CALBET and M. A. ALARIO-FRANCO, *ibid.* **B42** (1986) 167.
6. M. TANAKA, R. SAITO and K. TSUZUKI, *J. Phys. Soc. Jpn* **51** (1982) 2635.
7. V. S. STUBICAN, Paper presented at International Conference on Science and Technology of Zirconia, Tokyo, 1986.
8. V. P. DRAVID, unpublished research.
9. N. STENTON, MS thesis, Lehigh University (1982).
10. R. GEVERS, D. DELAVIGNETTE, H. BLANK and S. AMELINCKX, *Phys. Status Solidi* **4** (1964) 383.
11. J. W. EDINGTON, in "Practical Electron Microscopy in Materials Science", Micrograph No. 3 (Philips, Eindhoven, 1975).
12. R. GEVERS, P. DELAVIGNETTE, H. BLANK, J. VAN LANDUYT and S. AMELINCKX, *Phys. Stat. Solidi* **5** (1964) 595.
13. A. FOURDEUX, R. GEVERS and S. AMELINCKX, *ibid.* **24** (1967) 195.
14. H. L. BOWMAN, *Miner. Mag.* **15** (1908) 156.
15. H. F. KAY and P. C. BAILEY, *Acta Crystallogr.* **10** (1957) 219.

Received 13 March
and accepted 15 May 1987